Applied Physics A (2019) 125:579
https://doi.org/10.1007/s00339-019-2874-4

Applied Physics A
Materials Science & Processing

Optoelectronic characterization of CuInGa(S)$_2$ thin films grown by spray pyrolysis for photovoltaic application

Amal Bouich[1,2] · Bouchaib Hartiti[3] · Shafi Ullah[1] · Hanif Ullah[1] · Mohamed Ebn Touhami[2] · D. M. F. Santos[4] · Bernabe Mari[1]

Received: 16 February 2019 / Accepted: 25 July 2019 / Published online: 3 August 2019

Abstract
Copper–indium gallium disulfide (CIGS) is a good absorber for photovoltaic application. Thin films of CIGS were prepared by spray pyrolysis on glass substrates in the ambient atmosphere. The films were characterized by different techniques, such as structural, morphological, optical and electrical properties of CIGS films were analyzed by X-ray diffraction (XRD), scanning electron microscopy (SEM), atomic force microscopy (AFM), spectrophotometer and Hall effect, respectively. After optimization, the deposited films structure, grain size, and crystallinity became more important with an increase of annealing time at 370 °C for 20 min. Transmission electron microscopy (TEM) analysis shows that the interface sheets are well crystallized and the inter planer distance are 0.25 nm, 0.28 nm, and 0.36 nm. The atomic force microscopy (AFM) observation shows that the grain size and roughness can be tolerated by optimizing the annealing time. The strong absorbance and low transmittance were observed for the prepared films with a suitable energy bandgap about 1.46 eV. The Hall effect measurement system examined that CIGS films exhibited optimal electrical properties, resistivity, carrier mobility, and carrier concentration which were determined to be 4.22×10^6 Ω cm, 6.18×10^2 cm^2 V^{-1} S^{-1} and 4.22×10^6 cm^{-3}, respectively. The optoelectronic properties of CIGS material recommended being used for the photovoltaic application.

1 Introduction

Copper–indium gallium disulfide (CIGS) thin-film solar cells with a direct bandgap are already available in the market with a power conversion efficiency up to 23.8%, in the laboratory-scale which is very close to the silicon-based multi-crytalline solar cells [1]. To implement this technology, CIGS has a tuned bandgap of 1.04–1.68 eV depending on the gallium (Ga) content and has a high optical absorption coefficient of $\alpha > 10^5$ cm^{-1} [2]. To improve the efficiency of the cell, it is necessary to understand what parameter could affect the absorber layer performance [3].

Several techniques are developed to elaborate CIGS thin films such as sputtering [4], PVD [5], CVD [6], sol–gel [7], electrodeposition [8], co-evaporation [9], and pulsed laser [10]. Many efforts have been devoted to the developed alternative technique for elaboration of CIGS thin films using spray pyrolysis method. Spray pyrolysis and post-heat treatment are recognized as a promising low-cost method for the fabrication of CIGS absorber layers, based on their inherent advantages such as no requirement of expensive vacuum equipment, low cost, potentially suitable to obtain good quality and suitable for production large-area thin films economically [11]. A great amount of work has been published on sulfurization and salinization temperature. Few researchers give more details on the morphology and structures on the growth of CIGS thin films, especially in the temperature range from 200 to 400 °C [12].

In this work, we report low-cost spray pyrolysis method to synthesis CIGS films with different annealing times (5, 10 and 20 min). The films were characterized by X-ray diffraction (XRD), surface electron microscopy (SEM), energy-dispersive spectroscopy (EDS), transmission electron microscopy (TEM), atomic force microscopy (AFM), UV–Vis spectroscopy and with four-point probe method to

✉ Shafi Ullah
shafi399@yahoo.com

[1] Institut de Disseny I Fabricació, Universitat Politècnica de València, Camí de Vera s/n, 46022 Valencia, Spain

[2] Faculty of Sciences, LMEE Laboratory, BP 133, Kenitra, Morocco

[3] MAC&PM Laboratory, ANEPMAER Group FSTM, BP 146, Mohammedia, Morocco

[4] CeFEMA, IST-U, Lisbon, Portugal

Table 1 Parameters of XRD for sprayed CIGS films

Sample	Grain size (nm)	Dislocation density (/nm)	Lattice strain (ϵ)
Sprayed CIGS-1	429.82	5.41×10^{-6}	0.62
Sprayed CIGS-2	546.26	3.35×10^{-6}	0.56
Sprayed CIGS-3	567.22	3.10×10^{-6}	0.52

get an idea of the structural, morphology, optical and electrical properties of the thin films. The annealing temperature has a great impact on the optical, morphology and electrical properties of the films. The Hall effect has proved to be a convenient and useful tool for penetrating charge transport properties in the solid state and is routinely used as a standard material characterization method. The annealing time is the key factor of this work which is further discussed in detail in the "Results and discussion" with a constant annealing temperature 370 °C.

2 Experimental

The CIGS thin films were successfully deposited on glass substrates using a spray pyrolysis technique [13]. Spray technique involves preparing CIGS from electrolytic bath containing Cu–In–Ga–S elements in the form of $CuCl_2$, $InCl_3$, $GaCl_3$, and $SC(NH_2)_2$. Thin CIGS films were prepared using different precursors, $CuCl_2$ (1×10^{-2} M), $InCl_3$ (1×10^{-2} M), $GaCl_2$ (1×10^{-2} M) and $SC_2(NH_2)_2$ (3×10^{-2} M) as a sulfur source which were dissolved in distilled water. The substrate temperature was kept at 370 °C. Nitrogen (N_2) was used as the carrier gas, distance between the nozzle and substrate was set to 25 cm, and the spray rate was 1.0 ml min^{-1} with deposition time of 30 min [13].

During the spray, all parameters were fixed. Finally, the samples were rinsed under deionized water (DI) and dried at 60 °C in oven for 5 min, and for the crystallinity improvement, the as-deposited samples were annealed on the hot plate at 370 °C for different annealing times.

The crystal structure of CIGS at different annealing time (5, 10 and 20 min) composites were investigated by X-ray diffraction (XRD) using a Rigaku Ultima IV diffractometer in the Bragg–Brentano configuration using CuKα radiation ($\lambda = 1.54060$ Å). Chemical composition, surface morphology, and topography were characterized using energy-dispersive spectroscopy (EDS) and field emission scanning electron microscopy (FESEM), a Zeiss ULTRA 55 model equipped with an In-Lens SE detector, respectively.

Optical properties of the CIGS films were measured at room temperature using IR–Vis–UV spectrophotometer at a wavelength within the range 400–900 nm.

2.1 Lattice parameters

To calculate the lattice parameters [14], the following two equations could be used taking into consideration the following values: the angle 2θ and the value of the plane hkl correspondent:

$$\frac{1}{d^2} = \frac{h^2 + k^2}{a^2} + \frac{l^2}{c^2}, \tag{1}$$

$$n\lambda = d_{hk_l} \sin(\theta), \tag{2}$$

where a and c represent the lattice parameters, d_{hkl} is the lattice spacing of hkl. h,k, and l are the Miller indices, k is the wavelength of the CuK_α radiation (0.154 nm), and 2θ is the diffraction angle of the corresponding plane. After the calculation, we got the lattice parameters:

$a = 5.54$ Å and $c = 11.14$ Å.

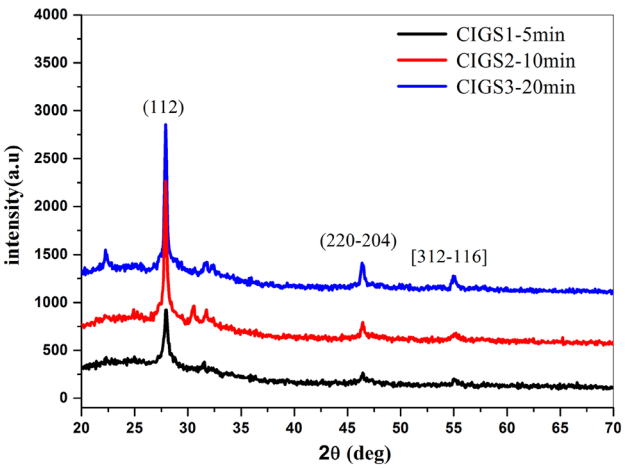

Fig. 1 XRD results for sprayed CIGS samples with different annealing time

Table 2 The deposition conditions of sprayed CIGS samples

Samples name	Annealing temperature (°C)	Pressure (bar)	Thickness (μm)	Annealing time (min)
Sprayed CIGS-1	370	2.5	2	5
Sprayed CIGS-2	370	2.5	2	10
Sprayed CIGS-3	370	2.5	2	20

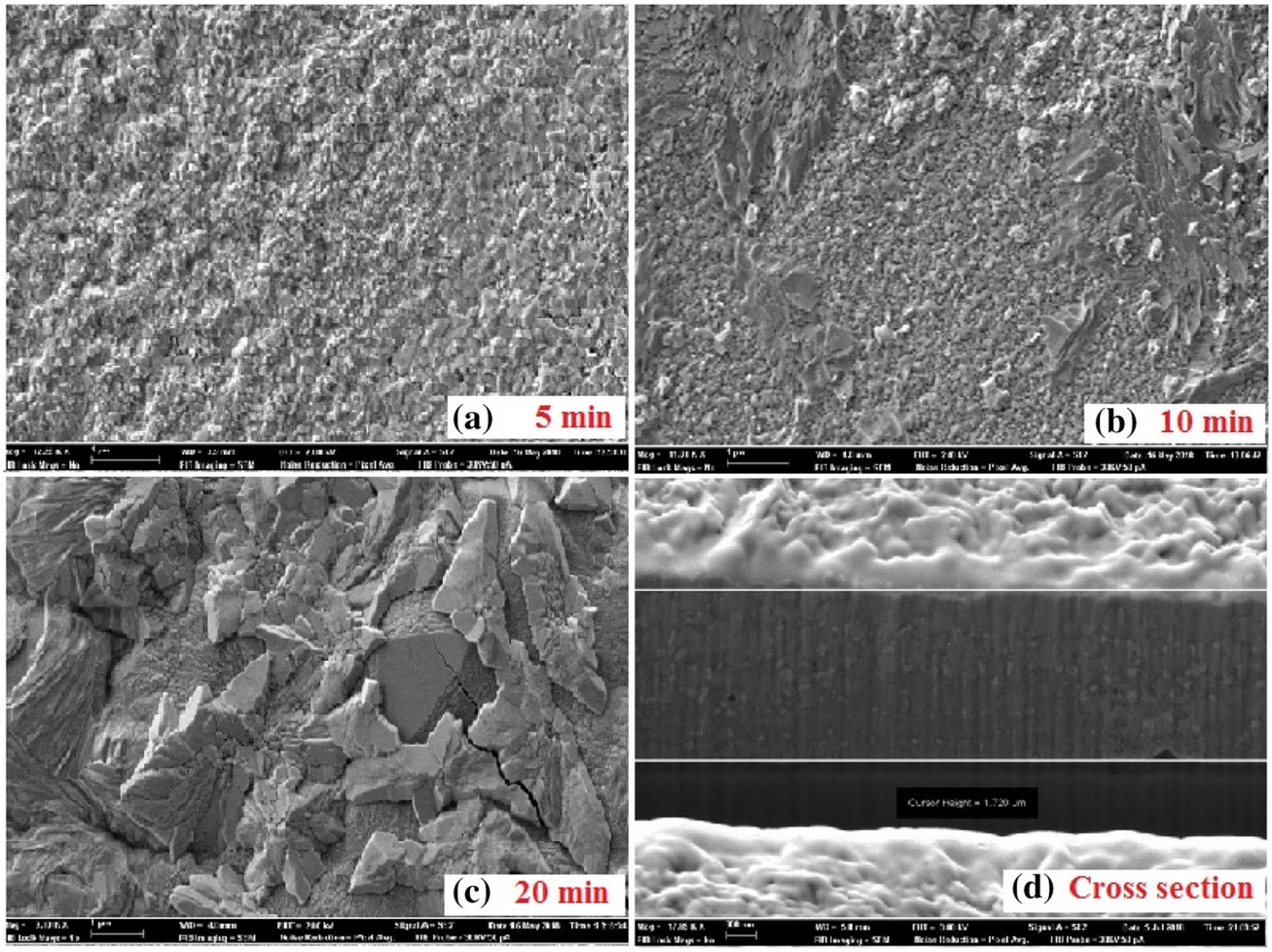

Fig. 2 SEM images with different annealing time: **a** CIGS-1 for 5 min, **b** CIGS-2 for 10 min, **c** CIGS-3 for 20 min and **d** cross-section for CIGS 20 min

2.2 Grain size and effective lattice strain

Effective lattice strain can give us an idea about the imperfections and deformations of the grains in the level of the thin layer sprayed, and for the calculation, we can use the following equation where it links the grain size with the effective lattice strain [15]. The grain size of the films sprayed CIGS increased from 2.8 to 7.67 nm with increase of annealing time (Table 1):

$$\beta \cos(\theta) = \frac{k\lambda}{D} + 4\varepsilon \sin(\theta), \tag{3}$$

where k is a constant whose value was taken as 0.94, k is the wavelength of X-ray used, β is the full-width half maximum (FWHM), θ is the Bragg angle, D is grain size and ε is the effective lattice strain.

2.3 Dislocation density

The dislocation density can be estimated by measurements made by transmission electron microscopy (TEM) which gives more precision on a specific area of the thin layer or by calculations from X-ray diffraction data (XRD) [16]. The dislocation density of the crystal was evaluated using the following formula [17], where γ is the dislocation density and D is the grain size of the thin films. The deposition condition of spayed CIGS thin films is presented in Table 2, where all the parameters are constant except annealing time (5, 10 and 20 min):

$$\gamma = {}^{1}/_{d^2}. \tag{4}$$

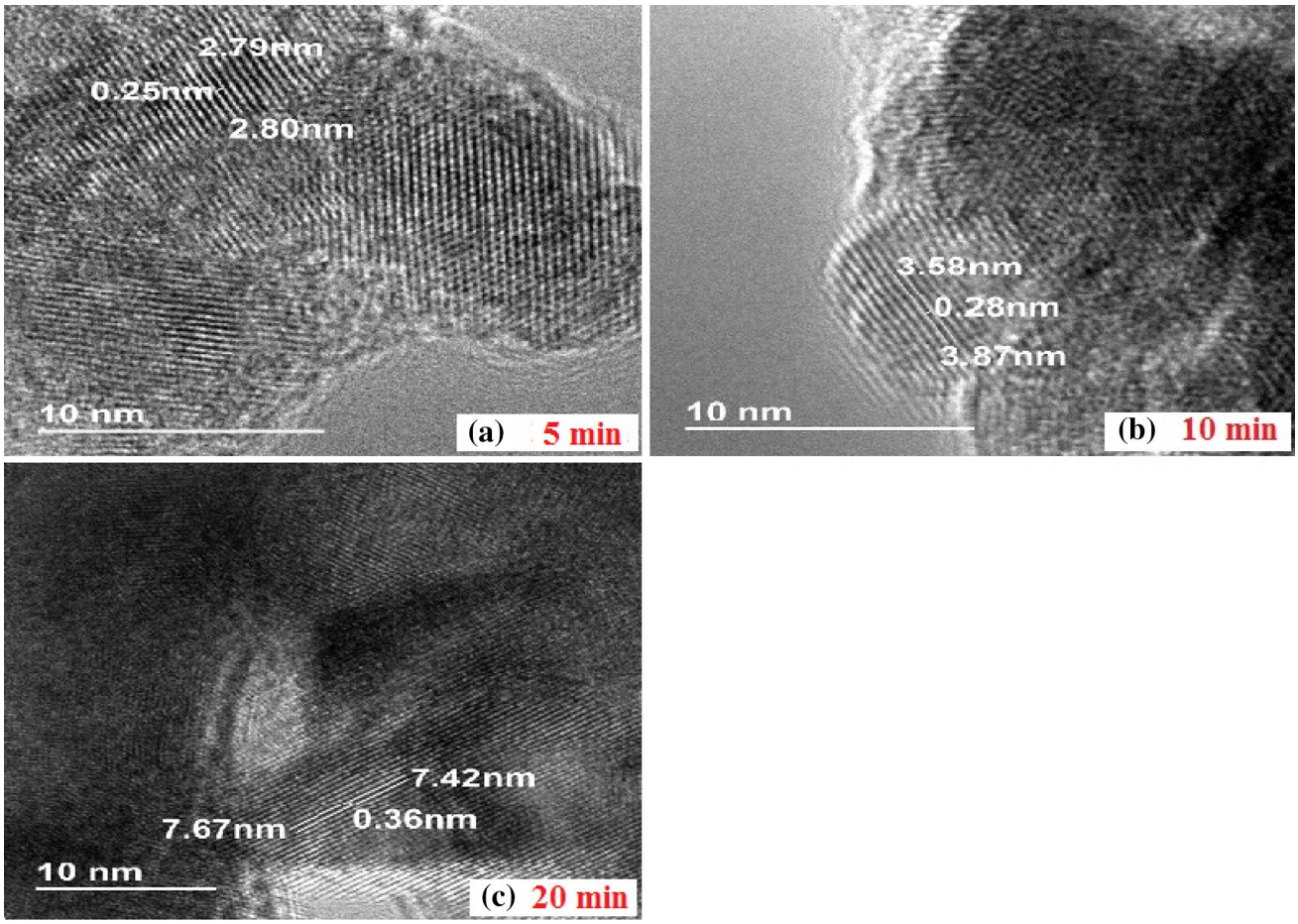

Fig. 3 TEM results **a** CIGS-1 for 5 min, **b** CIGS-2 for 10 min and **c** CIGS-3 for 20 min

3 Results and discussion

3.1 X-ray diffractogram (XRD) analysis

Figure 1 shows representative XRD peak with a chalcopyrite structure of the annealed CIGS samples. The major XRD peaks are observed to be oriented to [112, 220/204 and 312/116] diffraction planes. The pattern well matches with tetragonal structure JCPDS NO. 075-0104 corresponding to CIGS. The diffraction peaks confirm that the intensity of the peaks increases due to different annealing times (5, 10 and 20 min).

3.2 Scanning electron microscopy (SEM)

Figure 2 shows the surface morphology of the CIGS films sprayed with different annealing times. The variation in the grain size from 429 to 567 nm (Table 2) of the samples has been evident that the annealing time has an impact on it is an agreement with XRD results of Fig. 1. The samples treatment of the surface of the thin films at temperature 370 °C for 20 min plays an essential role for the enlargement of the grain size which has considerable importance for the effectiveness of the absorber layer.

3.3 Transmission electron microscopy (TEM)

Transmission electron microscopy is a direct method to have direct access to the size and shape of grains, and polydispersity of nanocrystals [18], and the images taken by transmission electron microscopy shows that inter-plane distance of the grains is becoming larger with the duration of surface treatment of the thin layers prepared by spray pyrolysis.

The surface treatment times 5 min, 10 min and 20 min of the samples increases the inter-planer distance of the samples to 0.25 nm, 0.28 nm, and 0.36 nm, respectively (see Fig. 3).

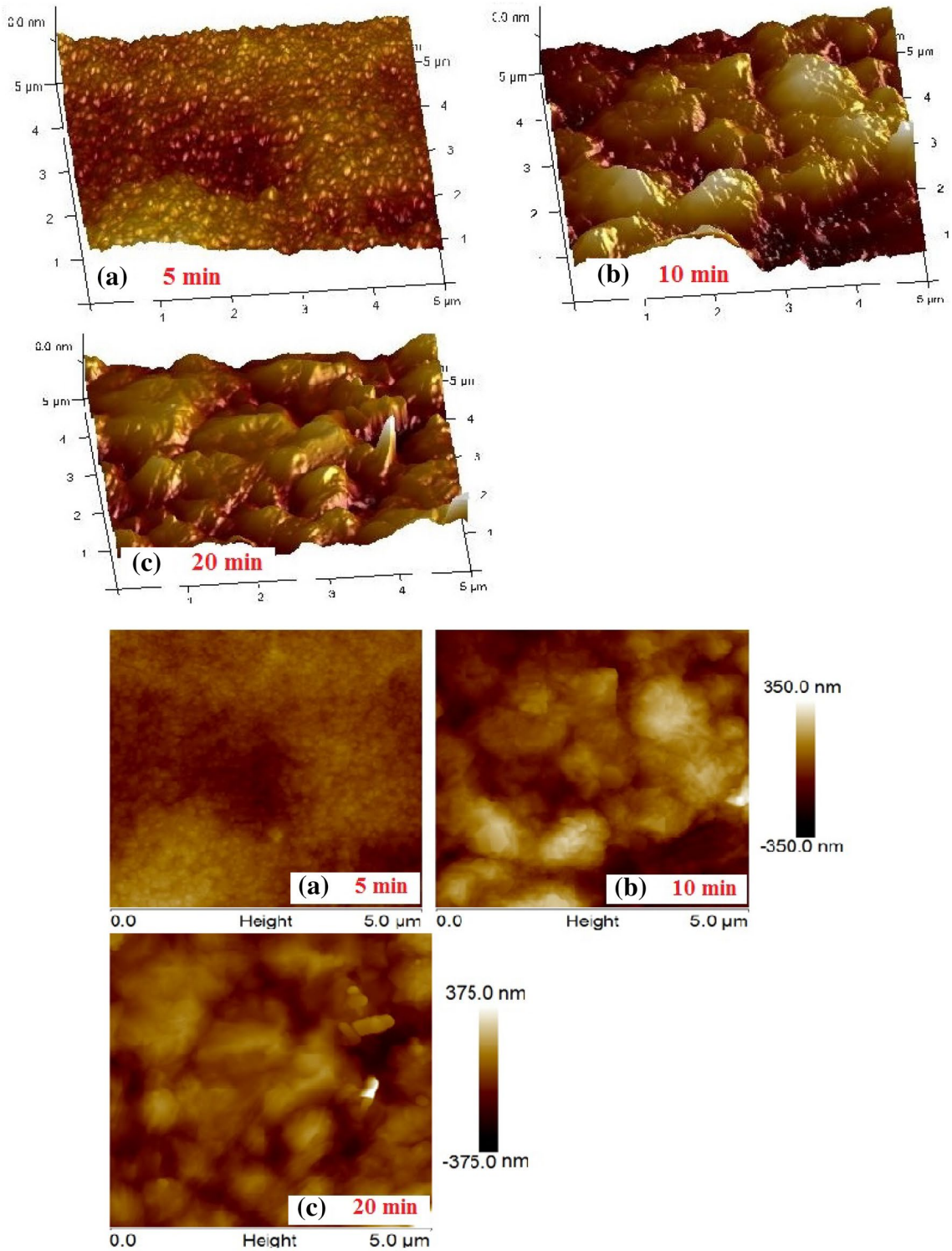

Fig. 4 2D and 3D AFM images of CIGS thin films: **a** CIGS-1 5 min, **b** CIGS-2 10 min and **c** CIGS-3 20 min

3.4 Atomic force microscopy (AFM)

Figure 4 shows the 2D and 3D surface topography with a difference in roughness and grain size of the films [19]. According to AFM analysis, annealing time affects the roughness and the grain size of the samples (Table 3). The grain boundaries of the films become low due to increasing grain size to reduce the recombination rate and increase the

Table 3 Roughness and grain size of CIGS thin films prepared by spray pyrolysis

Sample ID	Roughness (nm)	Grain size (nm)
Sprayed CIGS-1 5 min	318	429.82
Sprayed CIGS-2 10 min	490	546.26
Sprayed CIGS-3 20 min	751	567.22

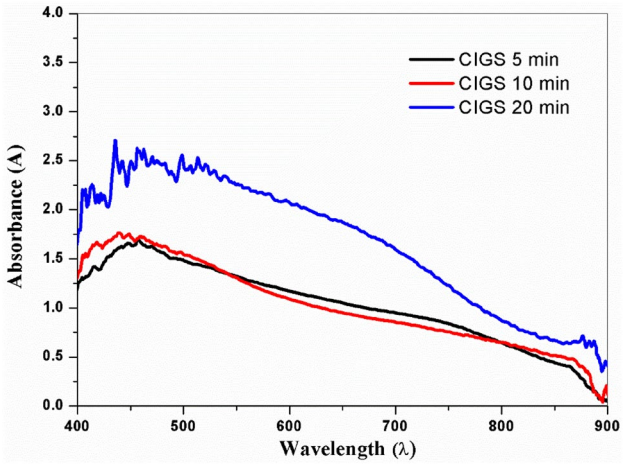

Fig. 5 The optical absorbance of the CIGS samples obtained by spray with annealing

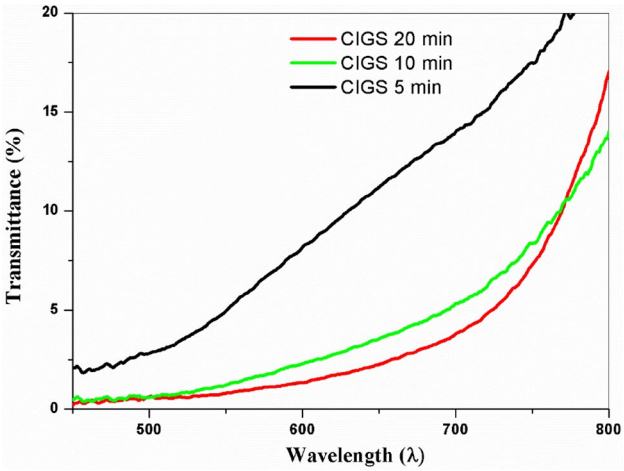

Fig. 6 Optical transmittance of the CIGS thin films

device performance, which is favorable for the performance of solar cells as the roughness increases to trap more light.

3.5 Optical properties

Annealing temperature and annealing time have a great impact on the optical properties and the optical constants

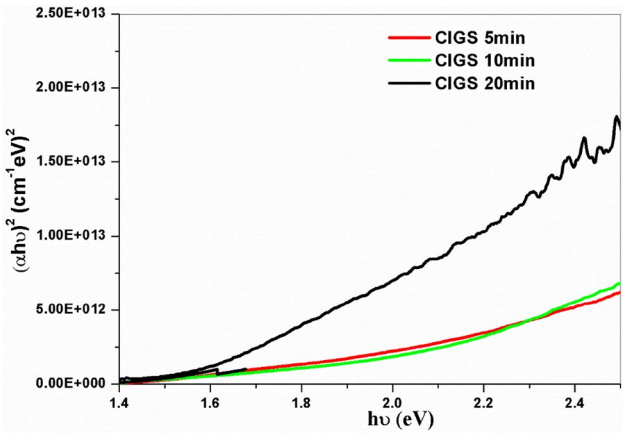

Fig. 7 The optical absorbance of the CIGS thin films

Table 4 Optical properties of the CIGS thin films

Precursor	n	k	ε_r	ε_i
Sprayed CIGS-1 15 min	4	0.03	12.5	0.25
Sprayed CIGS-2 10 min	4	0.03	12.5	0.25
Sprayed CIGS-3 20 min	5	0.04	14	0.37

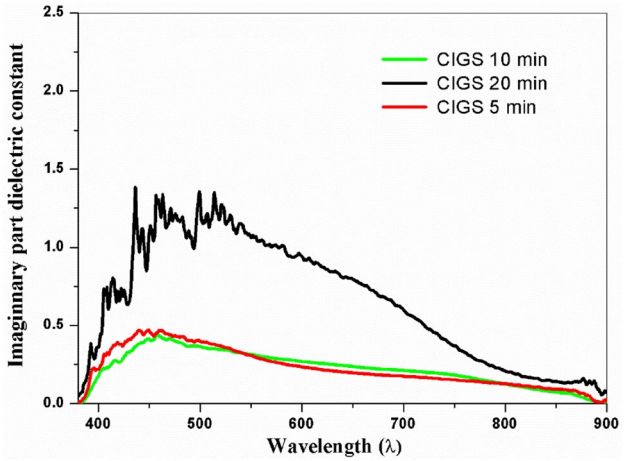

Fig. 8 The imaginary part dielectric constant of the CIGS thin films

which are very important for the efficiency of a semiconductor [20]. The absorbance in Fig. 5 shows the recorded absorption for the sprayed CIGS-3 sample treated at a 370 °C temperature for 20 min in the wavelength range 400–900 nm. It is found that all the films have a high absorbance and low transmittance. There is a small difference in the results in terms of percentage (%) of the absorbance and transmittance of the films. The highest transmittance value is observed for the CIGS-1 sprayed (25%) with annealing for 5 min and the CIGS-3 film with lower transparency of

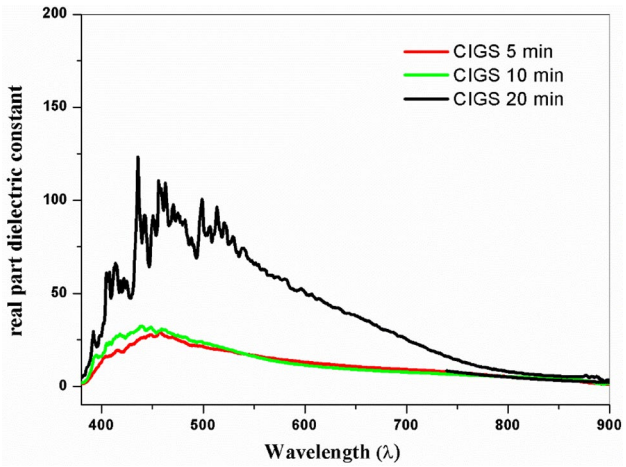

Fig. 9 The real-part dielectric constant of the CIGS thin films

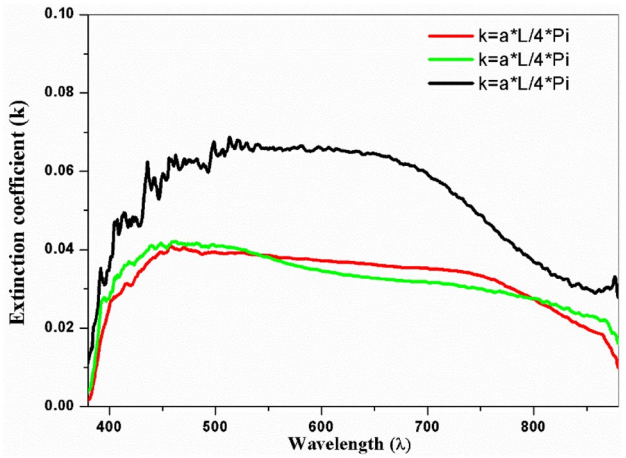

Fig. 10 The extinction coefficient of the CIGS thin films

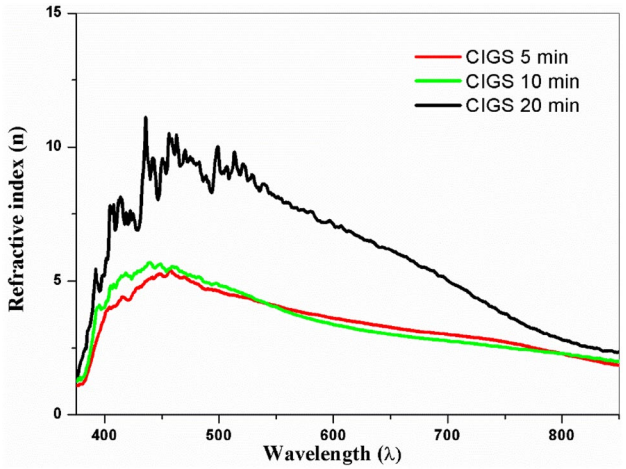

Fig. 11 Refractive index of the CIGS thin films

10% (Fig. 6). The data reveal that the increase in absorption and decrease in transmission with annealing time is related to improving grain size and roughness of the samples. The roughness of the surface played an important role to absorb more light that cause to improve the device performance.

By processing the slaps at a temperature 370 °C for 20 min shows high absorbance in the visible region with a maximum value of about 1.15.

To calculate the gap energy of the thin films prepared, we use the following equation and it concludes from the linear diagram of $(\alpha h\upsilon)^2$ versus $h\upsilon$ [21]:

$$(\alpha h\upsilon)^2 = B\left(h\upsilon - E_g\right), \tag{5}$$

where α is absorption coefficient calculated by Eq. (5), h is the Planck constant, B is a constant, E_g is the bandgap energy and t is the thickness of the thin film.

$$\alpha = \frac{1}{t}\ln\left(\frac{1}{T}\right). \tag{6}$$

The calculated values of bandgap energy are 1.66 eV for sample sprayed CIGS-1, 1.62 eV for sprayed CIGS-2. For sample sprayed CIGS-3, a strong absorbance and bandgap energy of the order of 1.46 eV make the films annealed at 370 ºC for 20 min a good choice for photovoltaic application [8] (see Fig. 7).

3.6 Optical constants

The optical constants, namely refractive index n, extinction coefficient (k), real part (ε_r) and imaginary part (ε_i) of dielectric constant for CIGS, are calculated using the following equations whose values are presented in Table 4 [22]:

$$n = \left(\frac{1+R}{1-R}\right) + \sqrt{\frac{4R}{(1-R)^2} - k^2}, \tag{7}$$

$$K = \frac{\alpha\lambda}{4\prod}, \tag{8}$$

$$\varepsilon_r = n^2 - k^2, \tag{9}$$

$$\varepsilon_i = 2nk, \tag{10}$$

where n is the refractive index, k is the extinction coefficient, λ is the wavelength, α is the absorption coefficient and R is the reflectance of the films. The value of the refractive index for the films sprayed is attributed to the thickness of the films. The high extinction coefficient value is observed for this sprayed CIGS-3 due to the high absorption into this film compared to the other samples. The high extinction coefficient values are attributed to the high absorbance of CIGS-3.

Table 5 Electrical properties of the CIGS thin films calculated using Van der Pauw method

Samples	Concentration (1 cm^{-3})	*Rs* (Ω sq^{-1})	*R* (10^{-2} Ω cm)	Conductivity (1 Ω cm)	Mobility (Cm^2 V s^{-1})
CIGS-1 5 min	1.5×10^{15}	404.40	606.60	2.5×10^{15}	6.87×10^{2}
CIGS-2 10 min	1.1×10^{16}	434.07	651.01	3.8×10^{15}	7.98×10^{1}
CIGS-3 20 min	1.2×10^{16}	435.01	652.60	0.8×10^{15}	8.74×10^{1}

Both real and imaginary parts of dielectric constant decrease with the wavelength and the maximum values are observed on the sample sprayed CIGS-3 (see Figs. 8, 9, 10, 11).

3.7 Electrical properties

Hall effect measurements gave us information about the electrical properties. Using four-point probe methods, electrical resistance is obtained using the following equation [13]:

$$R = R_s \times t, \tag{11}$$

where t is the thickness and R_s is the resistivity of the thin film.

The resistivity of the three thin layers is of the order of 10^{-2} Ω cm, the lowest resistivity value is observed for the annealed films where the resistivity in the orderd of 0.65 Ω cm for all the samples. The low values of resistivity are attributed to the electrical nature of CIGS semiconductors. The concentration and mobility of the charge carriers in the CIGS layers are determined by Hall effect measurements [23, 24]. The measurements made by the Hall effect allowed us to determine the resistivity (R_s) where we found that it is in the order of 10^{-2} Ω cm and the mobility (μ) is of the order 10^2 cm^2 V^{-1} s^{-1}, and for the concentration carriers (n), the order 10^6 1 cm^{-3}. The mobility (μ_n) and the concentration (n) of the charge carriers are listed in Table 5.

4 Conclusion

The CIGS thin films were prepared and deposited by spray pyrolysis technique and treated with a 370 °C annealing temperature at different annealing times. Thin films have been studied using several characterization techniques such as X-ray diffraction to calculate the lattice parameters, effective lattice strain, and dislocation density. Scanning electron microscopy (SEM) shows that the surface is with a noticeable difference in grain size. Transmission electron microscopy (TEM) results confirm the strong relation that films are polycrystalline.

Atomic force microscopy (AFM) shows outstanding relation with the grain size and roughness of the surface of the films. The high absorbance and low transmittance are observed for the films prepared with a bandgap energy of approximately 1.46 eV. Optical constants such as refractive index (n), extinction coefficient (k), real part (ε_r) and imaginary part (ε_i) of the dielectric constant were extracted by absorbance/transmittance data.

The carrier concentration, the mobility, resistivity and conductivity for the films treated at a 370 °C time for 20 min are 1.2×10^{16} 1 cm^{-3}, 652.60×10^{-2} Ω cm, 0.8×10^{15} 1 Ω cm^{-1}, 8.74×10^{-1} cm^2 V^{-1} S^{-1}, respectively. By considering the values found for the electrical properties, it is proposed that 20 min annealing under 370 °C temperature is an optimum choice for the CIGS solar cells.

Acknowledgements Prof. Bouchaib HARTITI, The Senior Associate at ICTP, is very grateful to ICTP for permanent support. Prof. Mohamed Ebn Touhami, Director of the University Center for Analysis, Expertise, Transfer of Technology and Incubation, Kenitra, Morocco, is very grateful to CUA2TI for financial support. Thanks to Doctor Diogo M.F. Santos for the supervision of Amal Bouich's work during her research in CeFEMA research center. The authors also thank researchers from CeFEMA (IST-ULisboa, Portugal) and CUA2TI (FS-Kenitra Morocco) for their help.

References

1. T. Feurer, P. Reinhard, E. Avancini, B. Bissig, J. Löckinger, P. Fuchs, S. Buecheler, Progress in thin film CIGS photovoltaics–Research and development, manufacturing, and applications. Prog. Photovolt. Res. Appl. **25**(7), 645–667 (2017)
2. A. Zegadi, M.A. Slifkin, M. Djamin, A.E. Hill, R.D. Tomlinson, A photoacoustic study of $CuIn_xGa_{1-x}Se_2$ alloys. Phys. Status Solidi (A) **133**(2), 533–540 (1992)
3. T.H. Sajeesh, A.R. Warrier, C.S. Kartha, K.P. Vijayakumar, Optimization of parameters of chemical spray pyrolysis technique to get n and p-type layers of SnS. Thin Solid Films **518**(15), 4370–4374 (2010)
4. J. Liu, D. Zhuang, H. Luan, M. Cao, M. Xie, X. Li, Preparation of Cu (In, Ga) Se_2 thin film by sputtering from Cu (In, Ga) Se_2 quaternary target. Progr. Nat. Sci. Mater. Int. **23**(2), 133–138 (2013)
5. M.I. Hossain, Fabrication and characterization of CIGS solar cells with In_2 S_3 buffer layer deposited by PVD technique. Chalcogenide Lett. **9**(5), 185–191 (2012)
6. M.A. Mughal, R. Engelken, R. Sharma, Progress in indium (III) sulfide (In_2S_3) buffer layer deposition techniques for CIS, CIGS, and CdTe-based thin film solar cells. Sol. Energy **120**, 131–146 (2015)
7. M. Powalla, M. Cemernjak, J. Eberhardt, F. Kessler, R. Kniese, H.D. Mohring, B. Dimmler, Large-area CIGS modules: Pilot line

production and new developments. Sol. Energy Mater Sol. Cells **90**(18–19), 3158–3164 (2006)
8. M.E. Calixto, P.J. Sebastian, R.N. Bhattacharya, R. Noufi, Compositional and optoelectronic properties of CIS and CIGS thin films formed by electrodeposition. Sol. Energy Mater. Sol. Cells **59**(1–2), 75–84 (1999)
9. S. Jung, S. Ahn, J.H. Yun, J. Gwak, D. Kim, K. Yoon, Effects of Ga contents on properties of CIGS thin films and solar cells fabricated by co-evaporation technique. Curr. Appl. Phys. **10**(4), 990–996 (2010)
10. S. R. Ovshinsky, X. Deng, R. Young, *U*.S. Patent No. 5,231,047. Washington, DC: U.S. Patent and Trademark Office (1993).
11. M. Kaelin, D. Rudmann, A.N. Tiwari, Low cost processing of CIGS thin film solar cells. Sol. Energy **77**(6), 749–756 (2004)
12. Fangdan Jiang, Jiayou Feng, Effect of temperature on selenization process of metallic Cu–In alloy precursors. Thin Solid Films **515**(4), 1950–1955 (2006)
13. S. Shirakata, Y. Kannaka, H. Hasegawa, T. Kariya, S. Isomura, Properties of Cu (In, Ga) Se_2 thin films prepared by chemical spray pyrolysis. Jpn. J. Appl. Phys. **38**(9R), 4997 (1999)
14. Y.K. Kumar, G.S. Babu, P.U. Bhaskar, V.S. Raja, Effect of starting-solution pH on the growth of Cu_2ZnSnS_4 thin films deposited by spray pyrolysis. Phys. Status Solidi (A) **206**(7), 1525–1530 (2009)
15. M. Ajili, M. Castagné, N.K. Turki, Characteristics of $CuIn_{1-x}Ga_xS_2$ thin films synthesized by chemical spray pyrolysis. J. Lumin. **150**, 1–7 (2014)
16. B.J. Babu, S. Velumani, A. Kassiba, R. Asomoza, J.A. Chavez-Carvayar, J. Yi, Deposition and characterization of graded Cu $(In_{1-x}Ga_x)$ Se_2 thin films by spray pyrolysis. Mater. Chem. Phys. **162**, 59–68 (2015)
17. S.F. Varol, G. Babür, G. Çankaya, U. Kölemen, Synthesis of sol–gel derived nano-crystalline ZnO thin films as TCO window layer: effect of sol aging and boron. RSC Adv. **4**(100), 56645–56653 (2014)
18. J.A. Frantz, R.Y. Bekele, V.Q. Nguyen, J.S. Sanghera, A. Bruce, S.V. Frolov, I.D. Aggarwal, Cu (In, Ga) Se_2 thin films and devices sputtered from a single target without additional selenization. Thin Solid Films **519**(22), 7763–7765 (2011)
19. C. Calderón, G. Gordillo, P. Bartolo-Pérez, F. Mesa, Effect of the deposition conditions on the optical, morphological and compositional properties of $CuIn_{1-x}Ga_xSe_2$ thin films prepared by a multistage process. Revista Mexicana de Física **53**(7), 270–273 (2007)
20. D. Schmid, M. Ruckh, F. Grunwald, H.W. Schock, Chalcopyrite/defect chalcopyrite heterojunctions on the basis of $CuInSe_2$. J. Appl. Phys. **73**(6), 2902–2909 (1993)
21. U.C. Matur, S. Akyol, N. Baydoğan, H. Cimenoglu, The optical properties of CIGS thin films derived by sol-gel dip coating process at different withdrawal speed. Proc. Soc. Behav. Sci. **195**, 1762–1767 (2015)
22. A. Bouich, B. Hartiti, S. Ullah, M.E. Touhami, B. Mari, D.M.F. Santos, Investigation of the optical properties of CuIn (Se, S)2 thin films for photovoltaic application. Mater. Today Proc. **13**, 663–669 (2019)
23. K. Matsumura, T. Fujita, H. Itoh, D. Fujita, Characterization of carrier concentration in CIGS solar cells by scanning capacitance microscopy. Meas. Sci. Technol. **25**(4), 044020 (2014)
24. A. Bouich, B. Hartiti, S. Ullah, H. Ullah, M.E. Touhami, D.M.F. Santos, B. Mari, Experimental, theoretical, and numerical simulation of the performance of CuInxGa(1–x) S2 based solar cells. Optik **183**, 137–147 (2019)